NEWS Integrated Analysis (NEWS-IA) Dataset: Budgets and Input Data		
Prepared By: J. Brent Roberts, NASA MSFC William S. Olson, GSFC/UMBC	**Revision**	Initial Version (V0)
	Date	November 20, 2024
Description: This documentation provides a summary of the underlying physical and mathematical descriptions of the global energy and water cycle budgets used to produce the NASA Energy and Water Cycle Study (NEWS) Integrated Analysis. In addition to discussion of the budget equations, a summary is provided concerning NEWS regions, input data sources, and data fields found in the NEWS-IA input data file.		

Document Revision History		
Revision	**Date**	**Changes**
Initial Version (V0)	November 20, 2024	N/A

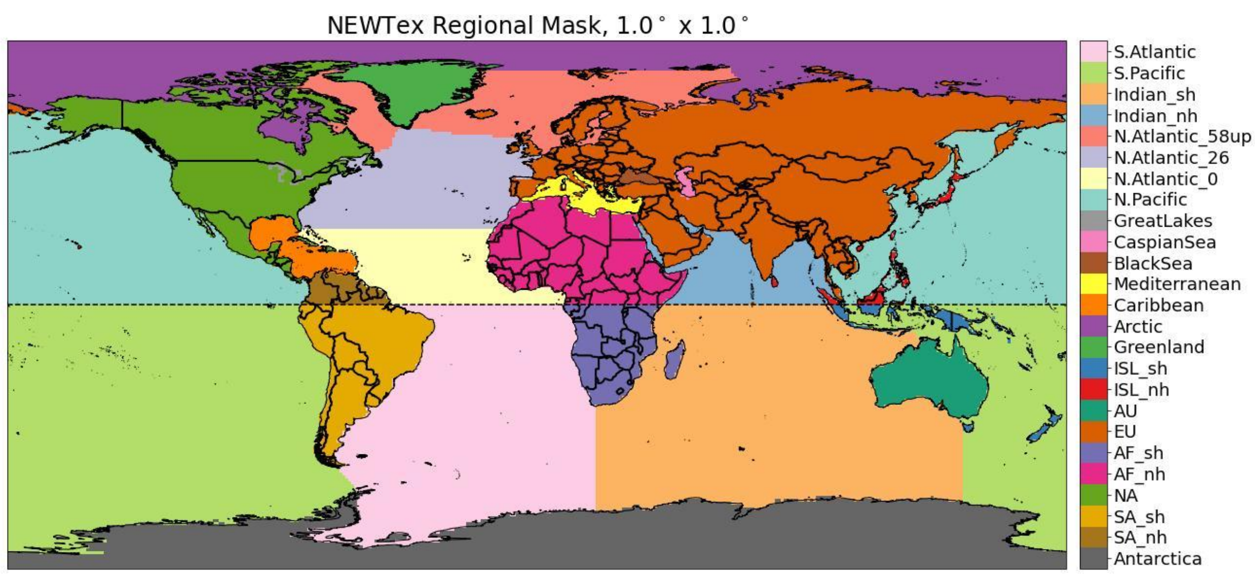

Table of Contents

Background

A series of projects conducted over multiple NASA Energy and Water Cycle Study (NEWS) funding cycles has resulted in the establishment and continued refinement of a water and energy budget optimization methodology. Application of this methodology has resulted in the NEWS climatologies of L'Ecuyer et al. (2015) and Rodell et al. (2015). The existing Version 1 NEWS climatology data are available from the GES DISC. An essential benefit of the budget optimization is the ability to close the water and energy budgets objectively and simultaneously, considering the uncertainties in the input remote sensing and model-based data products. The latest refinements to the budget optimization approach have enabled three fundamental advances: i) a fully integrated Earth system budget including the atmosphere, ocean, land surface, and cryosphere subsystems, ii) the ability to assess monthly-resolved time variability as opposed to a static climatology and iii) increased flexibility to address regional energy and water variability at finer spatial scales.

The primary outcome of this ongoing activity is the development and dissemination of the **NEWS Integrated Analysis (IA):** A historical, objectively optimized analysis of energy and water cycle budget components encompassing the storage and exchanges within and between the atmosphere, ocean, land surface, and cryosphere primarily based on NASA Earth Observations. The approach relies on a consistent treatment of Earth's energy and water budgets, linked through the latent heat fluxes. The optimization framework is designed to address transports across shared boundaries and to accommodate both random and systematic uncertainty. The budget optimization approach has been applied to 25 regions defined based on the goals and limitations of previous NEWS investigations, with refinements of and additions to the original set of regions. This dataset is appropriate for use in regional to global energy and water budget investigations. Limitations on the scale and number of regions are driven by factors including the effective resolution of observational datasets, uncertainties of the underlying datasets and other model optimization constraints (e.g., number of parameters, length of datasets, etc.).

Developing the optimized NEWS-IA dataset requires additional choices with respect to the development of Earth system energy and water balance budgets and, further, the selection and preprocessing of numerous input budget components from multiple remote sensing and model-based estimates. We have developed column-integrated budgets for different Earth subsystems including the atmosphere, land surface with storage layers (e.g., canopy, surface water, land ice and snow), and the ocean including sea ice. Treatment of the enthalpy exchanges associated with mass transfer across the atmosphere-surface interfaces is also included following recent development in the literature (e.g., Mayer et al., 2017; Trenberth and Fasullo, 2018). Additional considerations are necessary to implement an optimization framework and address uncertainty characterization and will be detailed in a future version of this document. Herein, the treatment of the Earth system budgets and the processing of input data sources for regional optimization are described.

Global Energy and Water Cycle Budgets

Variability of the climate system is driven by exchanges of mass and energy across a wide range of space and time scales and multiple Earth subsystems. These include variations within and between the atmosphere, land surface, cryosphere, and oceans. Radiative fluxes of energy supplied at the top of the atmosphere are responsible for supplying the forcing needed to drive the fluid motions, provide heating, and support the phase changes of water as it navigates through the global water cycle. Numerous activities are ongoing with a focus on developing estimates of the energy and water cycle components and characterizing their variations. These include efforts making using of a variety of in situ and remote sensing observations together with observation-constrained reanalyses and coupled modeling systems. Many budget constraint efforts have focused on individual Earth subsystems, but recent efforts are also focused on addressing the consistency of budget estimates across multiple elements. To support the NEWS-IA at regional scales, treatment of the Earth system begins with an emphasis on column-integrated budgets of the atmosphere, land, ocean, and surface storage layers (e.g., canopy, snow, sea ice). A detailed treatment and derivation of the budgets is available but well beyond the scope of the current document. In the following, we provide details of the simplified budget equations as used to support the budget optimization.

Atmospheric Mass and Energy Budgets

To construct a series of consistent atmospheric budgets for mass, momentum, and energy a prerequisite is to define a specific conceptual model for treatment of the atmosphere and its interaction with other systems within the Earth system. For NEWS-IA, the atmospheric system is assumed to be comprised of a multicomponent, multiphase mixture of dry (*d*) air, water vapor (*v*), cloud liquid (*l*) water, cloud ice (*i*) water, precipitating liquid (*r*) water (i.e., rain), and precipitating ice (*s*) water (i.e., snow). The system is considered open in that it is allowed to exchange both energy and mass with other components of the Earth system through its boundaries. All mass components are assumed to share the cloudy air mass horizontal velocity, $\boldsymbol{v_{c,h}}$, but precipitating particles may fall with their own relative (i.e., diffusional) vertical velocities. Often, as in Mayer et al. (2017) and Trenberth and Fasullo (2018), the assumption is made to neglect the contributions of liquid and ice condensate to both local storage rates and horizontal transports. This practice has been followed in the development of NEWS-IA budgets. The NEWS-IA optimization focuses on both total atmospheric mass and atmospheric water balances. Under the assumptions stated here, the column-integrated atmospheric water and mass budgets can be shown to take the following form:

$$\frac{\partial}{\partial t}\langle q_v \rangle + \nabla_h \cdot \langle \overrightarrow{\boldsymbol{v_{c,h}}} q_v \rangle = E_{atm} - P_r - P_s \tag{1}$$

$$\frac{1}{g}\frac{\partial p_s}{\partial t} + \nabla_h \cdot \langle \overrightarrow{\boldsymbol{v_{c,h}}} \rangle = E_{atm} - P_r - P_s \tag{2}$$

where q_v, is specific humidity (i.e., atmospheric water vapor), ∇_h is the horizontal divergence operator, E_{atm} is surface evaporation to the atmosphere, P_r is rainfall, P_s is snowfall, g is gravitational acceleration, and p_s is surface pressure. Angle brackets are used to denote the vertical integration of a parameter A from the top-of-atmosphere pressure (p_T) to the surface pressure:

$$\langle A \rangle = \frac{1}{g}\int_{p_T}^{p_s} A\, dp \tag{3}$$

Atmospheric energy can take the forms of potential, kinetic, and internal energy. Based on the atmospheric model as described above, and under the further assumption that all constituents are at the same atmospheric temperature, column-integrated budgets can be derived for total energy, dry energy, dry static energy, and moist static energy. Various “atmospheric energy” budgets have been used in energy budget studies. For example, static energy budgets are often used when authors opt to neglect contributions from kinetic energy. However, Trenberth et al. (2002) found the transports of kinetic energy to be on the order of 30-50Wm^{-2} in the storm track regions. While smaller than the moist static energy contributions, these are not insignificant for our purposes. The total energy equation — dry energy (i.e., including kinetic energy) plus moist energy — can be recovered through simple linear combination of a dry energy equation with a scaled version of the atmospheric water balance equation. For the NEWS-IA optimization framework, it is thus sufficient to consider the dry energy equation together with the above atmospheric mass budgets. For the NEWS-IA, the dry atmospheric energy budget takes the form:

$$\frac{\partial}{\partial t}\left\langle c_p(T-T_0)+K_t\right\rangle + \frac{\phi_s}{g}\frac{\partial p_s}{\partial t} + \nabla_h \cdot \left\langle \overrightarrow{\boldsymbol{v}_{\boldsymbol{c},\boldsymbol{h}}}\left(c_p(T-T_0)+K_t+\phi\right)\right\rangle = F_{R,sfc}^{T} - F_{R,toa}^{T} + F_{SH,sfc}^{T} + E_{atm}\left(c_{pv}(T_s-T_0)+\phi_s\right) - P_r\left(c_{pl}(T_w-T_0)+\phi_s\right) - P_s\left(c_{pi}(T_w-T_0)+\phi_s\right) + L_v(T_0)P_r + L_s(T_0)P_s \tag{4}$$

where c_p is the (variable) specific heat capacity at constant pressure of the atmospheric mixture, T is the atmospheric temperature, T_0 is the chosen reference temperature*, K_t is the total atmospheric kinetic energy, ϕ_s is the time-invariant surface geopotential energy, ϕ is the atmospheric geopotential energy, $F_{R,sfc}^{T}$ and $F_{R,toa}^{T}$ are the net (positive upward) radiative fluxes at the surface and top of atmosphere from all components, $F_{SH,sfc}^{T}$ is the upward sensible heat flux at the surface, c_{pk} is the (constant) specific heat capacity at constant pressure of constituent k, T_s is the surface temperature, T_w is the wet-bulb temperature at which rain and snow are assumed to be at the surface, $L_v(T_0)$, $L_f(T_0)$, and $L_s(T_0)$ are the latent heats of vaporization, fusion, and sublimation at the reference temperature. Arriving at this equation includes neglecting contributions of kinetic energy exchanges associated with mass transfer at the surface and uses the fact $\frac{\partial}{\partial t}\langle \phi_s \rangle = \frac{\phi_s}{g}\frac{\partial p_s}{\partial t}$ to explicitly include the surface pressure tendency in the energy budget equation. In this form, we explicitly include the often-neglected enthalpy exchanges associated with the surface mass exchanges. For completeness, scaling Equation (1) by $L_v(T_0)$ and combining with Equation (4), the total atmospheric energy equation becomes:

* For NEWS-IA, the reference temperature T_0 is chosen as 273.15K.

$$\frac{\partial}{\partial t}\langle c_p(T-T_0)+L_v(T_0)q_v+K_t+\phi_s\rangle+\nabla_h\cdot\langle\overrightarrow{\boldsymbol{v_{c,h}}}\big(c_p(T-T_0)+L_v(T_0)q_v+K_t+\phi\big)\rangle$$
$$=F^T_{R,sfc}-F^T_{R,toa}+F^T_{SH,sfc}+L_v(T_0)E_{atm}+L_f(T_0)P_s$$
$$+E_{atm}\big(c_{pv}(T_s-T_0)+\phi_s\big)-P_r\big(c_{pl}(T_w-T_0)+\phi_s\big)-P_s\big(c_{pi}(T_w-T_0)+\phi_s\big) \quad (5)$$

Note again, however, that the NEWS-IA optimization approach explicitly considers the dry energy budget (Equation 4) and atmospheric water balance (Equation 1) as separate budget constraints rather than constraining a single total energy equation. Further, note the use of surface pressure tendency in the dry energy budget. When developing the optimization approach, this form allows for a single state variable (surface pressure) to be accounted for in multiple budget constraints.

Terrestrial Water Storage

A region may generally encompass various model grid cells and/or physical hydrological basins that are comprised of a heterogenous landscape. The terrestrial water storage (TWS) is defined as the combination of water in all its various forms stored in the subsurface, vegetative canopies, snow and icepacks, and surface water storage elements including rivers, lakes, and floodplains. Developing a budget for the regional terrestrial water storage follows from application of the individual columnar land water budgets for various classes (e.g., bare soil, vegetated, snow, land ice, surface water). The change in TWS over a region is developed through area-integration of all individual columnar (i.e., per unit area) mass budgets. Combining the total land column budgets and interpreting the fluxes as their regional means (total mass flux per total area of region), the budget for terrestrial water storage change (TWSC) is formulated as:

$$\frac{\partial}{\partial t}TWS=TWSC=P_r+P_s-E_{atm}+\frac{\varrho_l}{A}\left(\mathrm{Q}^{\mathrm{T}}_{\mathrm{up,vol}}-\mathrm{Q}^{\mathrm{T}}_{\mathrm{down,vol}}\right)-Q^{ice}_{div} \quad (6)$$

where fluxes represent the regional mean over area A, $\mathrm{Q}^{\mathrm{T}}_{\mathrm{up,vol}}$ and $\mathrm{Q}^{\mathrm{T}}_{\mathrm{down,vol}}$ represent the total regional stream inflows and downstream outflows (in volumetric rate), and Q^{ice}_{div} is the area-average ice mass loss (i.e., glacier discharge). In the NEWS-IA budget implementation, additional efforts were undertaken to develop streamflow rates for the NEWS-IA computational grid using the HYMAP streamflow routing model. Thus, we make use of the TWSC equation as given by Equation (25). This is consistent with the optimization framework as it is designed to balance mass rates of change across grid cell and/or regional boundaries. Including routing is particularly necessary for NEWS-IA regions that have shared boundaries inland that may transect hydrologic basins.

Land Surface Energy Budget

As with the regional water budgets, land surface energy budgets can be developed through area-integration of energy budgets developed for each land surface class. The land surface energy budget addresses the storage and exchanges of energy with the atmosphere through radiative, conductive, and convective fluxes through the interfacial surface layer. The land surface energy budget has been described throughout the literature to varying degrees of complexity (de Vries, 1958; Milly, 1982; Jordan, 1991; Saito et al., 2006; and Sakai et al., 2011). For NEWS-IA, the land energy budget includes the storage of energy by different constituents, radiative and conductive processes, the latent heat exchanges associated with evaporative and freeze/melt processes, and enthalpy transports associated with movement of water throughout the system. Jordan (1991) and Jordan et al. (1999) provides an informative discussion and application of the conservation equations for a porous medium including extension to snow and ice layers. We will generally focus on the development of conservation equations that consider one-dimensional vertical flux exchanges. The developed land energy budget neglects vertical exchanges associated with dry air. All constituents within a layer are assumed to exist at the same local temperature, but precipitating constituents at the surface layer are assumed to be at the wetbulb temperature. All fluxes are defined with convention that positive fluxes are directed upwards (i.e., towards the atmosphere/out of the surface). This latter convention allows us to maintain consistency with the atmospheric energy budget previously developed. In addition to using a consistent reference temperature with that used for the atmospheric budget, we note that the choice of reference state for water is also arbitrary. Indeed, energy budgets describing only frozen soil and/or land ice/snow often use a reference state of solid ice at the freezing point (see Jordan, 1991). In such cases, latent energy terms associated with water transformation may appear of different sign from other budgets or be scaled by different latent heats (e.g., latent heat of sublimation). Given our focus on synergizing the atmospheric, land surface (including cryosphere), and oceanic budgets, we argue in favor of the use of a liquid water reference state. Both sensible and latent heat contributions are considered with respect to water and ice contents within the land column.

Under the stated assumptions and choice of reference state above, the total land energy budget over an arbitrary region comprised of a heterogenous landscape can be formulated as:

$$\frac{\partial H_{land}}{\partial t} = -F_{R,sfc}^{T} - F_{SH,sfc}^{T} - L_v(T_0)E_{atm} - L_f(T_0)P_s - E_{atm}\left(c_{pv}\left(T_s^{eff} - T_0\right) + \phi_s\right) + P_r\left(c_{pl}(T_w - T_0) + \phi_s\right) + P_s\left(c_{pi}(T_w - T_0) + \phi_s\right) - Q_{div}^{ice}\left(c_{pi}(T_{ice} - T_0) - L_f(T_0)\right) + \frac{\varrho_l}{A}\left(Q_{up,vol}^{T} - Q_{down,vol}^{T}\right)c_{pl}(T_{stream} - T_0) \tag{7}$$

where H_{land} is the total regional and column-integrated sensible and latent energy content arising from soils, vegetation (i.e., canopy biomass), snow, land ice, and surface water storage. Other parameters include T_s^{eff}, T_w, T_{ice}, and T_{stream} that describe the interfacial temperature, precipitating temperature (i.e., assumed as wetbulb temperature), temperature of snow and ice, and temperature of streams. These latter parameters all arise as part of accounting for energy loss related to enthalpy changes due to vertical and horizontal mass transfers. It is possible to develop direct estimates of H_{land} given knowledge of temperature profiles, assumptions on specific heat capacities of soils and vegetation types together with profiles of water mass, ice mass, and biomass content. Some of these elements can be estimated using remote sensing observations, but most state-of-the-art estimates rely on land surface modeling and applications of a closed surface energy balance to evolve the land energy storage field; and by relation, metrics such as the land surface temperature. This form of the land surface energy budget can be readily combined with the column-integrated atmospheric budget such that the vertical fluxes at the surface compensate. The total land-atmosphere budget for the area of interest then becomes:

$$\frac{\partial}{\partial t}\langle c_p(T-T_0)+L_v(T_0)q_v+K_t+\phi_s\rangle+\frac{\partial H_{land}}{\partial t}=-\nabla_h\cdot\langle\overrightarrow{\boldsymbol{v_{c,h}}}\left(c_p(T-T_0)+L_v(T_0)q_v+K_t+\phi\right)\rangle-F^T_{R,toa}-Q^{ice}_{div}\left(c_{pi}(T_{ice}-T_0)-L_f(T_0)\right)+\frac{\varrho_l}{A}\left(Q^T_{up,vol}-Q^T_{down,vol}\right)c_{pl}(T_{stream}-T_0) \quad (8)$$

In short, changes in the total energy storage for the combined land-atmosphere column are balanced by radiative fluxes at the top of the atmospheric column and lateral transports of energy through column-integrated atmospheric energy divergence, land ice and water transports.

Ocean and Sea Ice Energy and Mass Budgets

The ocean energy budget can be derived in a manner analogous to those of the atmosphere and land surface components. A primary difficulty that arises is the necessity of considering seawater in term of a mixture composition of freshwater and dissolved salts. The specific properties and thermodynamic potentials of seawater have been enumerated in the literature including the specification and adoption of international standards; for example, TEOS-10 (IOC et al. 2010). Considerable efforts have been undertaken recently to support the development of equations describing the conservation of energy and in a form that is consistent with the exchange of heat fluxes across the ocean surface. McDougall (2003) proposed the use of a "potential enthalpy" as a quantity that can be described using a conservation equation for energy to a very good approximation. This was further adopted and described in the TEOS-10 standard. As the oceanic community has traditionally made use of potential temperature in budget equations, a standard was developed to define the "conservative temperature", $\widehat{\Theta}$, as:

$$h_0=c_{p0}\widehat{\Theta} \quad (9)$$

where h_0 is the potential enthalpy and $c_{p0}\equiv 3991.86795711963$ (Jkg^{-1}K^{-1}) is the (defined) specific heat capacity of seawater that minimizes the difference between the conservative temperature and potential temperature at the ocean surface. It is defined with reference to (liquid) seawater at a reference temperature of $T_0=273.15K$ and is thus consistent with NEWS-IA reference state chosen for the atmosphere and land surface energy budgets. To a very good approximation, McDougall (2003) — and as further detailed in TEOS-10 standard (IOC et al., 2010) — the energy conservation equation can be written:

$$\frac{\partial\rho h_0}{\partial t}+\nabla\cdot(\rho\boldsymbol{v_o}h_0)=-\nabla\cdot\boldsymbol{F_Q} \quad (10)$$

where $\boldsymbol{v_o}$ is the seawater velocity, $\boldsymbol{F_Q}$ is heat flux by radiative, molecular conductive, and diffusional fluxes (both heat and salt), and we have neglected the dissipative effect of kinetic energy. Requiring consistency with the atmospheric budget, one may thus extend the ocean-atmosphere heat flux to include the additional fluxes of sensible enthalpy by the mass fluxes of evaporation, precipitation, and runoff. Neglecting the flux of salt at the ocean surface (e.g., ignoring the production of sea salt aerosols into the atmospheric boundary layer), we may vertically integrate the ocean energy budget over the ocean column from the bottom boundary, $z_b=-d$ (where d is ocean depth) in terms of potential enthalpy as:

$$\frac{\partial}{\partial t}\langle\rho c_{p0}\widehat{\Theta}\rangle_{ocean}=-\nabla_h\cdot\langle\rho c_{p0}\boldsymbol{v_{o,h}}\widehat{\Theta}\rangle_{ocean}-F^T_{rad,sfc}-F_{SH,sfc}-L_v(T_0)E_s-L_f(T_0)P_s-E_s\left(c_{pv}(T_s-T_0)+\phi_s\right)+P_r\left(c_{pl}(T_w-T_0)+\phi_s\right)+P_s\left(c_{pi}(T_w-T_0)+\phi_s\right)+\frac{\varrho_l}{A}Q^T_{in}\,c_{pl}(T_{stream}-T_0) \quad (11)$$

where the ocean heat content OHC is $\langle \rho c_{p0} \widehat{\Theta} \rangle_{ocean}$. This form explicitly accounts for energy changes related to the land surface transports for water and ice (i.e., rivers and glaciers), where Q_{in}^T is the total aggregated streamflow into the ocean region. Away from the coasts (i.e., where we neglect any runoff effects), the combined ocean-atmosphere column energy budget is thus:

$$\frac{\partial}{\partial t}\langle c_p(T - T_0) + L_v(T_0)q_v + K_t + \phi_s \rangle + \frac{\partial}{\partial t} OHC = -\nabla_h \cdot \langle \overrightarrow{\boldsymbol{v_{c,h}}} \left(c_p(T - T_0) + L_v(T_0)q_v + K_t + \phi \right) \rangle - \nabla_h \cdot \langle \rho c_{p0} \boldsymbol{v_{o,h}} \widehat{\Theta} \rangle_{ocean} - F_{R,toa}^T \quad (12)$$

The total energy change is thus driven by radiative fluxes at the top of the atmospheric column and the lateral fluxes of energy out of the atmospheric and oceanic columns. Note that this formulation is particularly defined for use of potential enthalpy using the conservative temperature. However, many ocean models continue to make use of potential temperature as the (approximately) conserved tracer. As the model budget equations are cast in forms consistent with use of potential temperature, the current recommendation is that model-derived budget components make use of the potential temperature rather than diagnosing the conservative temperature and recomputing storage and transports (see Griffies et al. 2016 for an extensive discussion). The NEWS-IA approach follows this recommendation to provide the unconstrained estimate of ocean heat content and transport.

In high-latitude regions, it is also necessary to consider the thermodynamics of sea ice in addition to the ice-free ocean. Mayer et al. (2019), for example, finds it important to consider the energy required to melt sea ice and impacts related to the movement of sea ice (see, Jordan et al., 1999). To support budgets at regional and monthly scales and with often-limited information on profiles of sea ice composition, additional assumptions are needed to develop tractable budgets. Constant snow and sea ice densities are assumed as is a constant specific heat capacity for snow and sea ice layers of depths h_i and h_{sn}. Further assuming a constant vertical-mean temperature, the sea-ice (with overlying snow) energy budget is specified as:

$$\begin{aligned}\rho_{si} c_{p,si} \frac{\partial}{\partial t}(T_{ice} - T_0)h_i - \rho_i^{si} L_f(T_0) \frac{\partial}{\partial t} h_i + \rho_{sn} c_{p,sn} \frac{\partial}{\partial t}(T_{sn} - T_0)h_{sn} - \rho_i^{sn} L_f(T_0) \frac{\partial}{\partial t} h_{sn} \\ = -\nabla_h \cdot \rho_{si} c_{p,si}(T_{ice} - T_0) h_i \boldsymbol{c_{i,h}} + \nabla_h \cdot \mathrm{L_f}(\mathrm{T_0}) \rho_{si} h_i \boldsymbol{c_{i,h}} - F_{R,h_{si}}^T - F_{SH,h_{si}}^T \\ - E_{h_{si}}\left(L_v(T_0) + c_{pv}(T_{sn} - T_0) + \phi_s \right) + P_{r,h_{si}}\left(c_{pl}(T_w - T_0) + \phi_s \right) + P_{s,h_{si}}\left(c_{pi}(T_w - T_0) - \right. \\ \left. L_f(T_0) + \phi_s \right) + Q_{div}^{ice}\left(c_{pi}(T_{ice} - T_0) - L_f(T_0) \right)\end{aligned} \quad (13)$$

where the left-hand side represents the tendency of total sensible and latent energy storage of the sea ice, H_{ice}. These storage changes are balanced by the lateral divergence of sensible and latent heat transports associated with sea ice motion characterized by $\boldsymbol{c_{i,h}}$, the radiative and turbulent heat fluxes impinging at the top of the sea ice/snow layer and their associated enthalpy changes. The last time accounts for energy changes associated with glacial ice discharge into the ocean and sea-ice column. There are additional fluxes associated with energy exchanges at the bottom of the sea ice with the underlying ocean (e.g., basal melt). We have not included these here as they are compensated when considering the total ocean and sea ice budget together within the column; it is this combined ocean and sea ice budget which is of direct interest to this study. For the NEWS-IA, multiple ocean modeling products provide information on the estimated sea ice mass and sea ice motion. These estimates are used to apply equation (32) to account for sea ice contributions to the ocean energy budget. In short, the total ocean and sea ice energy budget is given:

$$\frac{\partial}{\partial t}(OHC + H_{ice}) = -\nabla_h \cdot \langle \rho c_{p0} \boldsymbol{v_{o,h}} \widehat{\Theta} \rangle_{ocean} - \nabla_h \cdot \rho_{si} c_{p,si}(T_{ice} - T_0) h_i \boldsymbol{c_{i,h}} + \left(\nabla_h \cdot \mathrm{L_f}(\mathrm{T_0}) \rho_{si} h_i \boldsymbol{c_{i,h}}\right)_{si} - F^T_{R,sfc} - F^T_{SH,sfc} - L_v(T_0) E_{sfc} - L_f(T_0) P_s - E_{sfc}\left(c_{pv}\left(T_{sfc} - T_0\right) + \phi_s\right) + P_r\left(c_{pl}(T_w - T_0) + \phi_s\right) + P_s\left(c_{pi}(T_w - T_0) + \phi_s\right) + \frac{\varrho_l}{A} Q^T_{in}\, c_{pl}(T_{stream} - T_0) + Q^{ice}_{div}\left(c_{pi}(T_{ice} - T_0) - L_f(T_0)\right) \tag{14}$$

A set of coupled balance equations, mediated through the vertical exchanges between the atmosphere and surface, is completed through inclusion of the ocean and sea ice mass budgets. Both Griffies (2018) and Griffies (2009) provide an extensive development and discussion of ocean mass and volume budgets commonly used to support ocean modelling and diagnostics. Neglecting any internal sources and sinks of mass as well as salt fluxes at the surface, and integrating over the depth of the ocean as for the energy budgets, the column-integrated ocean mass (M) budget can be derived as:

$$\frac{\partial}{\partial t}\langle \rho \rangle_{ocean} = \frac{\partial M}{\partial t} = -\nabla_h \cdot \langle \rho \boldsymbol{v_{o,h}} \rangle_{ocean} + P_r + P_s - E_{atm} + \frac{\varrho_l}{A} Q^T_{in} \tag{15}$$

where ρ is the seawater density. The total mass change is balanced by column-integrated mass divergence, sources of mass from precipitation and total river runoff, and loss from surface evaporation. Following the prior development and assumptions necessary for sea ice energy balance, a the columnar mass of a layer of sea ice and snow (M_{ice}) covering the ocean surface can be described as:

$$\rho_{si} \frac{\partial h_i}{\partial t} + \rho_{sn} \frac{\partial h_{sn}}{\partial t} = \frac{\partial M_{ice}}{\partial t} = -\nabla_h \cdot \rho_{si} h_i \boldsymbol{c_{i,h}} - E_{h_{si}} + P_{r,h_{si}} + P_{s,h_{si}} + Q^{ice}_{div} \tag{16}$$

where we explicitly denote the vertical fluxes occurring at the top of the sea ice and snowpack h_{si}. We neglect sea ice runoff and basal melt here, again, as they are assumed to discharge into the ocean and will be compensated in a total column budget accounting for both ocean and sea ice. The sea ice mass balance within a column is thus governed by the supply of precipitation, mass convergence of sea ice, glacial ice mass, and loss through surface evaporation/sublimation processes. Together, the total ocean and sea ice mass budget is:

$$\frac{\partial M + M_{ice}}{\partial t} = -\nabla_h \cdot \langle \rho \boldsymbol{v_{o,h}} \rangle_{ocean} - \nabla_h \cdot \rho_{si} h_i \boldsymbol{c_{i,h}} + P_r + P_s - E_{atm} + \frac{\varrho_l}{A} Q^T_{in} + Q^{ice}_{div} \tag{17}$$

From the perspective of total surface mass budgets, the land surface TWSC balance can be combined with the ocean surface budgets. Along coastal regions, there will be a compensation of land-based glacial ice discharge into the ocean as well as the river (and subsurface) runoff.

Regional Budgets for Optimization

The balance conditions for atmospheric water, mass, and energy, as well as balance conditions for land surface water and energy, ocean mass and energy, are encompassed by equations (1), (2), (4), (6), (7), (14), and (17), respectively. These equations are generally isomorphic — functionally, they relate storage changes within either a column, or through integration to regional averages, to the lateral divergence (i.e. outward transports) of mass or energy — either over individual columns or across regional boundaries — and vertical fluxes at the upper and lower boundaries. Applying these budgets as individual constraints within the NEWS-IA optimization framework requires additional care and some assumptions to minimize the number of parameters that must be solved and to address potential nonlinearities. The parameters to be optimized are considered as part of a state vector. The individual budget terms within the balance constraints define the state variables. In theory, these budgets can be coupled at a variety of spatial and temporal scales. For example, one could consider constraining all budget components for individual grid scales (e.g., a 1x1 degree grid cell). Such an approach would require solving for 64800xN_v parameters where N_v is the total number of state variables contained with the budget constraints. Further, the lateral transports naturally couple the systems of equations spatially and increase the challenge of numerical optimization. To address these issues, the NEWS-IA generates constrained budget component estimates over a much smaller set of regions. Given a region of the Earth with area A_{region}, the balance conditions that apply to the bulk average mass/water/energy properties of that region are described as follows. Note that the mass balance constraints include scaling by L_v[†] such that they are comparable to those used in the energy budgets.

Multiplying the atmospheric mass balance condition by the latent heat of vaporization, to put all quantities in energy units, and then integrating over the area of the region,

$$\iint_{A_{region}} \left\{ \frac{L_v}{g} \frac{\partial p_s}{\partial t} + L_v\, P_r + L_v\, P_s - L_v\, E_{atm} \right\} da = -\oint_C L_v \left\langle \overrightarrow{\boldsymbol{v}_{c,h}} \right\rangle \bullet \hat{\boldsymbol{n}}\, dl \qquad (18)$$

Here, da is an incremental area element, $\overrightarrow{\boldsymbol{v}_{c,h}}$ is the horizontal wind vector at the boundary of the region, and dl is an incremental boundary length element. The unit normal $\hat{\boldsymbol{n}}$ points outward from the region at the boundary. We have applied Green's theorem to transform the area-integrated divergence to a line integral along the region boundary C.

The corresponding atmospheric water balance condition is

$$\iint_{A_{region}} \left\{ L_v \frac{\partial \langle q_v \rangle}{\partial t} + L_v\, P_r + L_v\, P_s - L_v\, E_{atm} \right\} da = -\oint_C L_v \left\langle q_v \overrightarrow{\boldsymbol{v}_{c,h}} \right\rangle \bullet \hat{\boldsymbol{n}}\, dl \qquad (19)$$

where we note $\langle q_v \rangle$ is total columnar water vapor. The balance for atmospheric energy follows as

$$\begin{aligned} \iint_{A_{region}} \Bigg\{ & \frac{\partial \langle c_p(T - T_0) + K_t \rangle}{\partial t} + \frac{\Phi_s}{g}\frac{dp_s}{dt} - F^T_{R,sfc} + F^T_{R,toa} - F^T_{SH,sfc} \\ & + L_v\, P_r \left\{ c_{pl}\,(T_w - T_o) + \Phi_s - L_v \right\}/L_v \\ & + L_v\, P_s \left\{ c_{pi}\,(T_w - T_o) + \Phi_s - L_s \right\}/L_v \\ & - L_v\, E_{atm} \left\{ c_{pv}\,(T_s - T_o) + \Phi_s \right\}/L_v \Bigg\} da \\ & = -\oint_C \left\langle \left\{ c_p(T - T_0) + K_t + \Phi \right\} \overrightarrow{\boldsymbol{v}_{c,h}} \right\rangle \bullet \hat{\boldsymbol{n}}\, dl \end{aligned} \qquad (20)$$

[†] Here, we drop notation on the dependence of latent heats on the reference temperature T_0.

where it should be noted that the surface precipitation and evaporation terms include scaling by L_v such that the terms $L_v P_r$, for example, represent the state variable as opposed to simply P_r.

The surface water balance of the combined surface storage/subsurface is given as:

$$\iint_{A_{region}} \left\{ L_v \frac{\partial TWS}{\partial t} - L_v\, P_r - L_v\, P_s + L_v\, E_{atm} \right\} da = -\oint_C L_v \langle \boldsymbol{F_{tw}} \rangle \bullet \boldsymbol{\hat{n}}\, dl \tag{21}$$

where $\boldsymbol{F_{tw}}$ is the total horizontal water mass flux directed outward along the region. For NEWS-IA, $\boldsymbol{F_{tw}}$ is estimated in land regions as the mass rate of streamflow crossing regional boundaries. Further, note that the ocean mass balance is structured analogous to the terrestrial water balance and can be applied at a regional scale by adjusting the TWS term to include ocean and sea ice mass, and $\boldsymbol{F_{tw}}$ to include column-integrated ocean and sea ice mass transports. Land and ocean mass budgets are currently treated as separate balance constraints, but future efforts may treat the surface mass balance as a single constraint.

The surface energy budget can likewise be cast into analogous forms for both land surface and ocean budgets. For NEWS-IA, we have shown above the potential for sensible and latent energy transfers associated with river runoff and glacier ice discharge. However, these are expected to be small and we lack reliable information on stream temperatures. The NEWS-IA balance conditions do not currently incorporate these as balance terms. Thus, a general surface energy balance condition can be written:

$$\begin{aligned}
\iint_{A_{region}} \Bigg\{ & \frac{\partial \langle OHC + H_{ice} + H_{land} \rangle}{\partial t} + F^T_{R,sfc} \\
& + F^T_{SH,sfc} + L_v\, E_{atm} \left\{ c_{pv}\, (T_s - T_o) + \Phi_s + L_v \right\} / L_v \\
& - L_v\, P_r \left\{ c_{pl}\, (T_w - T_o) + \Phi_s \right\} / L_v - L_v\, P_s \left\{ c_{pi} (T_w - T_0) + \Phi_s - L_f \right\} / L_v \Bigg\} da \\
& = - \oint_C \langle \boldsymbol{F_{oe}} + \boldsymbol{F_{ie}} \rangle \bullet \boldsymbol{\hat{n}}\, dl
\end{aligned} \tag{22}$$

where $\boldsymbol{F_{oe}} + \boldsymbol{F_{ie}}$ denote the outward directed ocean and sea ice energy transports. Note that without inclusion of energy transports by land surface water (i.e., rivers, glaciers), the land surface energy balance only includes vertical exchanges with the atmosphere. To be clear, the land-only surface energy budget for a region is then:

$$\begin{aligned}
\iint_{A_{region}} \Bigg\{ & \frac{\partial \langle H_{land} \rangle}{\partial t} + F^T_{R,sfc} + F^T_{SH,sfc} + L_v\, E_{atm} \left\{ c_{pv}\, (T_s - T_o) + \Phi_s + L_v \right\} / L_v \\
& - L_v\, P_r \left\{ c_{pl}\, (T_w - T_o) + \Phi_s \right\} / L_v - L_v\, P_s \left\{ c_{pi} (T_w - T_0) + \Phi_s - L_f \right\} / L_v \Bigg\} da \\
& = 0
\end{aligned} \tag{23}$$

Equations (18) – (23) provide the concise set of balance conditions used to develop NEWS-IA optimized budgets. However, it is still necessary to transform these mathematical descriptions into a more compact form that connects to variables specified in the NEWS-IA data files. Here, Table 1 explicitly defines the relationship between budget terms and data variables.

Table 1. List of NEWS-IA Variables and Budget Terms

NEWS-IA Variable	Budget Term	Units
AREA	A_{region}	m^2
PSTEND	$\frac{\partial p_s}{\partial t}$	Pa s^{-1}
QVTEND	$\frac{\partial \langle q_v \rangle}{\partial t}$	kg m^{-2} s^{-1}
HTEND	$\frac{\partial \langle c_p(T - T_0) \rangle}{\partial t}$	W m^{-2}
KTEND	$\frac{\partial \langle K_t \rangle}{\partial t}$	W m^{-2}
LES	$\frac{\partial H_{land}}{\partial t}$	W m^{-2}
OES	$\frac{\partial OHC + H_{ice}}{\partial t}$	W m^{-2}
SES	$\frac{\partial OHC + H_{ice} + H_{land}}{\partial t}$	W m^{-2}
TS	T_s	K
WETBULB	T_w	K
PHIS	Φ_s	m^2 s^{-2}
PRECIP	$P_r + P_s$	kg m^{-2} s^{-1}
RAIN	P_r	kg m^{-2} s^{-1}
SNOW	P_s	kg m^{-2} s^{-1}
RADTOA	$F^T_{R,toa}$	W m^{-2}
RADSFC	$F^T_{R,sfc}$	W m^{-2}
SHF	$F^T_{SH,sfc}$	W m^{-2}
EVAP	E_{atm}	kg m^{-2} s^{-1}
TWSC	$TWSC + \frac{\partial M + M_{ice}}{\partial t}$	kg m^{-2} s^{-1}
TWSC_LAND	$TWSC$	kg m^{-2} s^{-1}
TWSC_OCEAN	$\frac{\partial M + M_{ice}}{\partial t}$	kg m^{-2} s^{-1}
BOUNDARYLENGTH	C	m
DISCHARGE‡	$\oint_C \boldsymbol{F_{tw}} \bullet \boldsymbol{\hat{n}}\, dl$ (streamflow component, positive only)	kg s^{-1}

‡ Discharge represents the integrated mass transport computed from routed river runoff along each regional boundary directed positive from the source region to the destination region. For balance constraints, the net river runoff along a boundary is what is necessary and is derived from Discharge. For an inland regional boundary, it is possible for rivers to be flowing in different directions across different parts of the boundary.

TRANSPORT_MASS	$\oint_C \langle \overrightarrow{\boldsymbol{v}_{c,h}} \rangle \bullet \hat{\boldsymbol{n}}\ dl$	kg s^{-1}
TRANSPORT_QV	$\oint_C \langle q_v \overrightarrow{\boldsymbol{v}_{c,h}} \rangle \bullet \hat{\boldsymbol{n}}\, dl$	kg s^{-1}
TRANSPORT_H	$\oint_C \langle \{c_p(T - T_0)\} \overrightarrow{\boldsymbol{v}_{c,h}} \rangle \bullet \hat{\boldsymbol{n}}\, dl$	W
TRANSPORT_K	$\oint_C \langle K_t \overrightarrow{\boldsymbol{v}_{c,h}} \rangle \bullet \hat{\boldsymbol{n}}\, dl$	W
TRANSPORT_PHI	$\oint_C \langle \Phi \overrightarrow{\boldsymbol{v}_{c,h}} \rangle \bullet \hat{\boldsymbol{n}}\, dl$	W
TRANSPORT_OCEAN_HEAT	$\oint_C \langle \boldsymbol{F_{oe}} + \boldsymbol{F_{ie}} \rangle \bullet \hat{\boldsymbol{n}}\, dl$	W
TRANSPORT_SURFACE_ENERGY[§]	$\oint_C \langle \boldsymbol{F_{oe}} + \boldsymbol{F_{ie}} \rangle \bullet \hat{\boldsymbol{n}}\, dl$	W
TRANSPORT_OCEAN_MASS	$\oint_C \langle \rho \boldsymbol{v_{o,h}} \rangle_{ocean} \bullet \hat{\boldsymbol{n}}\, dl$	kg s^{-1}
TRANSPORT_LANDWATER_MASS	$\oint_C \boldsymbol{F_{tw}} \bullet \hat{\boldsymbol{n}}\, dl$ (net streamflow)	kg/s
TRANSPORT_SURFACE_MASS	$\oint_C (\langle \rho \boldsymbol{v_{o,h}} \rangle_{ocean} + \boldsymbol{F_{tw}}) \bullet \hat{\boldsymbol{n}}\, dl$	kg/s

With the definitions established in Table 1, we can reformulate the balance constraints into a form more directly amenable for use in the optimization framework. Noting that the optimization will make use of extensive properties of energy and mass fields, and that storage and vertical fluxes represent regional area-averages, the balance conditions for each region becomes:

$$(AMS + R + S - E)xAREA + AMF = 0 \quad (24)$$

$$(AWS + R + S - E)xAREA + AWF = 0 \quad (25)$$

$$(AES - RADSFC + RADTOA - SHF + \Gamma_\Phi AMS + \Gamma_r R + \Gamma_s S - \Gamma_e E)xAREA + AEF = 0 \quad (26)$$

$$(SWS - R - S + E)xAREA + SWF = 0 \quad (27)$$

$$(SES + RADSFC + SHF - \Gamma_r' R - \Gamma_s' S + \Gamma_e' E)xAREA + SEF = 0 \quad (28)$$

Additional notation in support of equations (24)-(28) are given in Table 2.

[§] Currently, the only lateral transports of surface energy are those due to ocean heat transports.

Table 2. List of budget terms and description of balance conditions used in optimization.

Budget Term	Definition	Description
AMS	$\frac{L_v}{g}\frac{dp_s}{dt}$	Atmospheric mass storage change
R	$L_v\, P_r$	Rain rate
S	$L_v\, P_s$	Snow rate
E	$L_v\, E_{atm}$	Evaporation rate
AMF	$L_v \oint_C \langle \overrightarrow{\boldsymbol{v_{c,h}}} \rangle \bullet \hat{\boldsymbol{n}}\ dl$	Atmospheric mass horizontal flux
AWS	$L_v \frac{\partial \langle q_v \rangle}{\partial t}$	Atmospheric water storage change
AWF	$L_v \oint_C \langle q_v \overrightarrow{\boldsymbol{v_{c,h}}} \rangle \bullet \hat{\boldsymbol{n}}\, dl$	Atmospheric water horizontal flux
AES	$\frac{\partial \langle c_p(T-T_0) + K_t \rangle}{\partial t}$	Atmospheric energy storage change
AEF	$\oint_C \langle \{c_p(T-T_0) + K_t + \Phi\} \overrightarrow{\boldsymbol{v_{c,h}}} \rangle \bullet \hat{\boldsymbol{n}}\, dl$	Atmospheric energy horizontal flux
SWS	$L_v(TWSC + \frac{\partial M + M_{ice}}{\partial t})$	Surface total water storage change
SWF	$L_v \oint_C (\langle \rho \boldsymbol{v_{o,h}} \rangle_{ocean} + \boldsymbol{F_{tw}}) \bullet \hat{\boldsymbol{n}}\, dl$	Surface total water horizontal flux
SES	$\frac{\partial OHC + H_{ice} + H_{land}}{\partial t}$	Surface energy storage change
SEF	$\oint_C \langle \boldsymbol{F_{oe}} + \boldsymbol{F_{ie}} \rangle \bullet \hat{\boldsymbol{n}}\, dl$	Surface energy horizontal flux
Γ_Φ	Φ_s / L_v	Mass scaling factor
Γ_r	$\overline{\{c_{pl}\,(T_w - T_o) + \Phi_s - L_v\}/L_v}$	Rain enthalpy and latent factor
Γ_s	$\overline{\{c_{pl}\,(T_w - T_o) + \Phi_s - L_s\}/L_v}$	Snow enthalpy and latent factor
Γ_e	$\overline{\{c_{pv}\,(T_s - T_o) + \Phi_s\}/L_v}$	Evaporation enthalpy factor
Γ_r'	$\overline{\{c_{pl}\,(T_w - T_o) + \Phi_s\}/L_v}$	Rain enthalpy factor
Γ_s'	$\{c_{pi}\,(T_w - T_o) + \Phi_s - (L_f)\}/L_v$	Snow enthalpy and latent factor
Γ_e'	$\overline{\{c_{pv}\,(T_s - T_o) + \Phi_s + L_v\}/L_v}$	Evaporation enthalpy and latent factor

The factors Γ_k are treated as constants that are maintained at their observed values in the current study, because the variable portions of these factors are relatively small compared to the constant latent heats, and keeping the factors constant makes the associated energy terms linear in R, S, E.

Data Analysis

Ensuring consistent computation of the vertically integrated budgets requires careful attention to the numerical techniques employed. We need to address the vertical integration, budget discretization and associated grids, identification of constants, and specification of direct and derived budget fields. Previous efforts including Trenberth et al. (1991), Trenberth et al. (2002), Mayer et al. (2017), and Mayer et al. (2021) have addressed several of the aspects related to accurate computation of the budgets. We summarize the approaches to each of the noted elements in the following.

Data Inventory

The production of the optimized NEWS-IA requires a complete set of initial (i.e., unadjusted) energy and water cycle budget terms covering all regions. A primary focus of the NEWS-IA project is to integrate the numerous products generated as part of the NASA Earth observing and modelling efforts. In Table 3, we provide a list of the source data products that have been selected for use as inputs to the NEWS-IA optimization. These include several of the latest versions of radiative, precipitation and evaporation fluxes, mass storage fields from GRACE, and both storage and transport estimates of mass and energy from model-based atmospheric, land surface, and ocean analyses.

Table 3. NASA Earth observation and modelling products that serve as inputs for the NEWS-IA.

Data Product	Terms	Temporal Coverage	Product Info / Data Access
Edition 4.2 CERES-EBAF	Top-of-Atmosphere and Surface Radiative Fluxes	03/2000 - 12/2023	CERES Data Products
GPCP Version 3.2	Precipitation	01/1983 - 12/2023	GPCP Data Access
SeaFlux Version 3	Ocean Evaporation	01/1988 - 12/2018	Data and Documentation
GRACE / GRACE-FO	Terrestrial Water Storage Change, Ocean Mass Change	04/2002 - Present	GRACE Data Portal
GLDAS-2.2 / GRACE-DA	Land Surface Water and Energy Storage, Land Evaporation, and Routed Streamflow	02/2003 - Present	GLDAS-2.2 Data Access
ECCO V4r4	Oceanic Energy Storage and Horizontal Transports, Sea Ice	01/1992 - 12/2017	ECCO Latest

MERRA-2	Atmospheric Dry Mass, Water, and Energy Storage and Horizontal Transports, Land Ice	01/1980 - Present	MERRA-2 Overview

Vertical Integration, Temporal Averaging and Discretization

For NEWS-IA, we examine the monthly-resolved energy and mass balances. For many of the budget parameters, we must use model reanalysis estimates of state variables including seawater density, temperature, humidity, velocity, and geopotential. While many reanalyses provide archives of these variables on standard pressure levels, the most accurate computations of the vertically integrated budgets are accomplished using data stored on native model vertical coordinate levels. Trenberth et al. (2002) note that the budgets are most accurately computed by applying vertical integration at the model time step and then carrying out time-averaging. Following prior studies, all computations requiring vertical integration are performed using model level native coordinates at the finest archived resolution available prior to any temporal averaging to the monthly resolution. For storage quantities, the required estimates are temporal derivatives. Because several of the modeling datasets are run at fine temporal resolution, direct estimation of the storage changes often includes large changes due to high-frequency variability that is not of direct interest to this study. To partially mitigate this issue, storage terms are computed using the last day of the previous month and the first day of a given month. This 2-day average (centered at the start of a month) of storage quantities is used to estimate the storage rate of change over each month based on simple differencing.

Spatial Domain, Discretization, and Resampling

The list of data sources identified in Table 3 provide energy and water cycle budget components on a set of disparate grids. They span specific domains — e.g., ocean-only, land-only, atmosphere — with generally inconsistent partitioning of land/ocean masking. These differences are in addition to inconsistencies in spatial grid resolution and alignment. To reconcile energy and water cycle budget constraints, it is required to develop estimates over consistent domains. For NEWS-IA, the global domain is discretized onto an equal-angle grid covering 90S to 90N and from 180W to 180E at a spatial resolution of 1 degree by 1 degree. Each grid cell is bounded on the side by integer degrees in longitude and latitude (e.g. -180, 179, -178, etc.). For each grid cell, the area contained with the appropriate quadrangle is computed for an ellipsoidal Earth following the WGS84 model and the lengths of all grid cell edges are stored.

Next, resampling and area-averaging of quantities must be addressed. There are three fundamental types of data variables to consider. These include local storage rates, vertical fluxes at the surface and top of the atmosphere, and horizontal transports. All vertical flux estimates and local storage terms are resampled to the NEWS-IA grid using area-weighted (i.e., conservative) resampling. This approach is consistent with those approaches used to address coupling between various modeling elements as developed within the Earth System Modeling Framework.

For terms involving the horizontal transports, however, additional efforts are needed. For any arbitrary 1x1 NEWS-IA grid cell, the grid northern, eastern, southern, and western boundaries may generally intersect a variety of surface classes. That is, only partial lengths of boundaries may be relevant for surface horizontal transports. Further, computing transports along the grid boundary edges requires an approach that can account for general lack of alignment between model grid cell edges and those of the 1x1 NEWS-IA cells. To address both of these issues, all 1x1 grid cell edges are discretized at a resolution of 1/120 degree consistent with the GLCC V2.0 land cover classification. All grid pixels along an edge are identified as representing an ocean-only, land-only, or mixed ocean/land boundaries. All transports are resampled using an inverse distance weighting scheme that includes contribution from the computed horizontal gradients of the zonal and meridional transports. Atmospheric transports are resampled to all discretized pixels along each grid cell boundary/edge. Oceanic transports are resampled to those pixels that are along ocean boundaries. For the land surface, only routed streamflow is currently treated as a lateral transport. The outputs of the routing schemed are used to identify into which region (and from each source region) streamflow is output.

NEWS Regions

The original NEWS energy and water cycle climatology of L'Ecuyer et al. (2015) and Rodell et al. (2015) focused on the description of the climatological energy and water balances for different global regions. The updated descriptions of these cycles are now focused on incorporating time-variability and scaling of the optimization towards a gridded product. However, it is prudent to begin with a similar regional focus as an incremental step towards a potential gridded objective analysis. The regional budgets, alone, provide important information for summarizing the large-scale storage, transports, and surface-atmosphere exchanges between land/ocean, continents, ocean basins, and cross-equatorial transports. Figure 1 identifies the 25

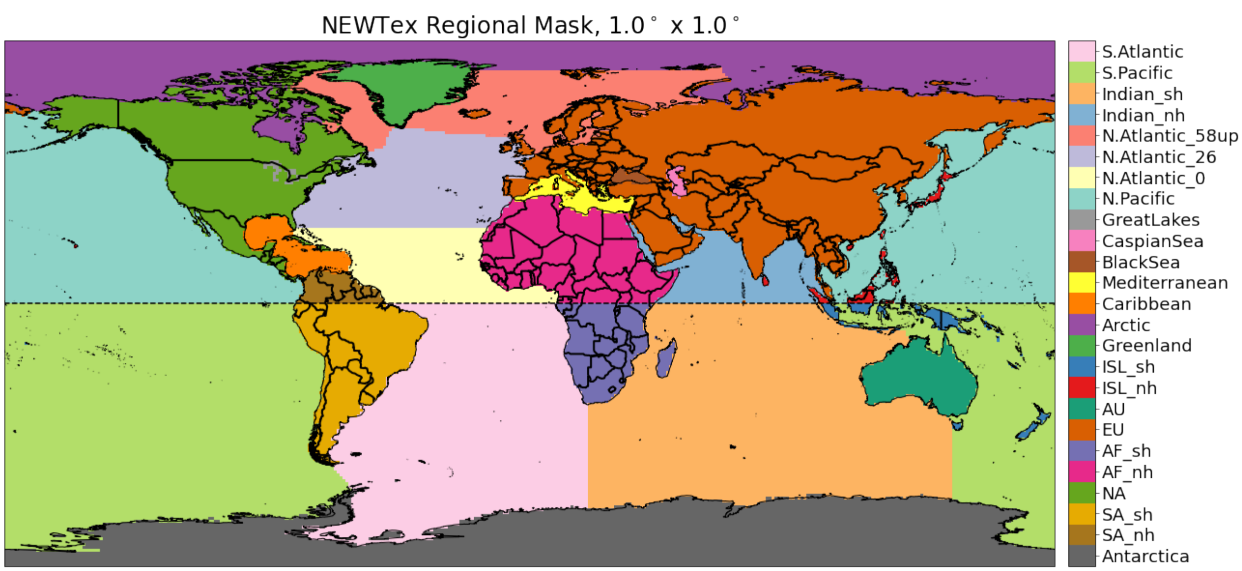

Figure 1. The partitioning of the Earth into 25 regions is shown as used for developing regionally balanced energy and water cycle budgets.

regions used for estimating regional budgets. Broadly, the northern and southern hemispheres are separated as are the major continental landmasses, and inland lakes and seas. The Atlantic Ocean basin is further separated across latitudes associated with observation-based ocean energy transport transects to be used for supporting evaluation of the quality of the heat transport estimates. To compute regional budgets, the 1x1 degree harmonized storage rates and vertical fluxes are regionally averaged while the transports are integrated along all shared regional boundaries. These regionally averaged fields, following the theory and pratical definitions and development described in the preceding sections provide the input data stored in the NEWS-IA V0 input data file and supplied to the optimization algorithm.

References

De Vries, D. A. (1958). Simultaneous transfer of heat and moisture in porous media. *Eos, Transactions American Geophysical Union*, *39*(5), 909-916.

Griffies, Stephen. *Fundamentals of ocean climate models*. Princeton university press, 2018.

Griffies, S. M., Danabasoglu, G., Durack, P. J., Adcroft, A. J., Balaji, V., Böning, C. W., Chassignet, E. P., Curchitser, E., Deshayes, J., Drange, H., Fox-Kemper, B., Gleckler, P. J., Gregory, J. M., Haak, H., Hallberg, R. W., Heimbach, P., Hewitt, H. T., Holland, D. M., Ilyina, T., … Yeager, S. G. (2016). OMIP contribution to CMIP6: Experimental and diagnostic protocol for the physical component of the Ocean Model Intercomparison Project. Geoscientific Model Development, 9(9), 3231–3296. https://doi.org/10.5194/gmd-9-3231-2016

Griffies, S. M., Schmidt, M. A. R. T. I. N., & Herzfeld, M. I. K. E. (2009). Elements of mom4p1. *GFDL Ocean Group Tech. Rep*, *6*, 444.

Intergovernmental Oceanographic Commission. (2015). The International thermodynamic equation of seawater–2010: calculation and use of thermodynamic properties.

Jordan, R. E. (1991). A one-dimensional temperature model for a snow cover: Technical documentation for SNTHERM. 89.

Jordan, R. E., Andreas, E. L., & Makshtas, A. P. (1999). Heat budget of snow-covered sea ice at North Pole 4. Journal of Geophysical Research: Oceans, 104(C4), 7785–7806. https://doi.org/10.1029/1999jc900011

Kato, S., Loeb, N. G., Fasullo, J. T., Trenberth, K. E., Lauritzen, P. H., Rose, F. G., Rutan, D. A., & Satoh, M. (2021). Regional energy and water budget of a precipitating atmosphere over ocean. Journal of Climate, 34(11), 4189–4205. https://doi.org/10.1175/JCLI-D-20-0175.1

L'Ecuyer, T. S., Beaudoing, H. K., Rodell, M., Olson, W., Lin, B., Kato, S., Clayson, C. A., Wood, E., Sheffield, J., Adler, R., Huffman, G., Bosilovich, M., Gu, G., Robertson, F., Houser, P. R., Chambers, D., Famiglietti, J. S., Fetzer, E., Liu, W. T., … Hilburn, K. (2015). The observed state of the energy budget in the early twenty-first century. Journal of Climate, 28(21), 8319–8346. https://doi.org/10.1175/JCLI-D-14-00556.1

Marquet, P. (2015). On the computation of moist-air specific thermal enthalpy. Quarterly Journal of the Royal Meteorological Society, 141(686), 67–84. https://doi.org/10.1002/qj.2335

Mayer, J., Mayer, M., & Haimberger, L. (2021). Consistency and homogeneity of atmospheric energy, moisture, and mass budgets in ERA5. Journal of Climate, 34(10), 3955–3974. https://doi.org/10.1175/JCLI-D-20-0676.1

Mayer, M., Haimberger, L., Edwards, J. M., & Hyder, P. (2017). Toward consistent diagnostics of the coupled atmosphere and ocean energy budgets. Journal of Climate, 30(22), 9225–9246. https://doi.org/10.1175/JCLI-D-17-0137.1

Mayer, M., Tietsche, S., Haimberger, L., Tsubouchi, T., Mayer, J., & Zuo, H. A. O. (2019). An improved estimate of the coupled Arctic energy budget. Journal of Climate, 32(22), 7915–7934. https://doi.org/10.1175/JCLI-D-19-0233.1

Mcdougall, T. J. (2003). Potential Enthalpy: A Conservative Oceanic Variable for Evaluating Heat Content and Heat Fluxes.

Milly, P. C. D. (1982). Moisture and heat transport in hysteretic, inhomogeneous porous media: A matric head-based formulation and a numerical model. *Water Resources Research*, *18*(3), 489-498.

Rodell, M., Beaudoing, H. K., L'Ecuyer, T. S., Olson, W. S., Famiglietti, J. S., Houser, P. R., Adler, R., Bosilovich, M. G., Clayson, C. A., Chambers, D., Clark, E., Fetzer, E. J., Gao, X., Gu, G., Hilburn, K., Huffman, G. J., Lettenmaier, D. P., Liu, W. T., Robertson, F. R., … Wood, E. F. (2015). The observed state of the water cycle in the early twenty-first century. Journal of Climate, 28(21), 8289–8318. https://doi.org/10.1175/JCLI-D-14-00555.1

Rodell, M., Chao, B. F., Au, A. Y., Kimball, J. S., & Mcdonald, K. C. (2005). Global Biomass Variation and Its Geodynamic Effects: 1982-98. http://EarthInteractions.org

Saito, H., Šimůnek, J., & Mohanty, B. P. (2006). Numerical Analysis of Coupled Water, Vapor, and Heat Transport in the Vadose Zone. Vadose Zone Journal, 5(2), 784–800. https://doi.org/10.2136/vzj2006.0007

Sakai, M., Jones, S. B., & Tuller, M. (2011). Numerical evaluation of subsurface soil water evaporation derived from sensible heat balance. Water Resources Research, 47(2). https://doi.org/10.1029/2010WR009866

Trenberth, K. E. (1991). Climate Diagnostics from Global Analyses: Conservation of Mass in ECMWF Analyses. Journal of Climate, 4(7), 707–722. https://doi.org/10.1175/1520-0442(1991)004<0707:CDFGAC>2.0.CO;2

Trenberth, K. E., & Fasullo, J. T. (2018). Applications of an updated atmospheric energetics formulation. Journal of Climate, 31(16), 6263–6279. https://doi.org/10.1175/JCLI-D-17-0838.1

Trenberth, K. E., Stepaniak, D. P., & Caron, J. M. (2002). Accuracy of Atmospheric Energy Budgets from Analyses. Journal of Climate, 15(23), 3343–3360. https://doi.org/10.1175/1520-0442(2002)015<3343:AOAEBF>2.0.CO;2

Appendix A. Constants

The constants required for budget estimates include not only gravity but also the specific heat capacities of atmospheric constituents and latent heats associated with water phase transformation. Each of these are defined with respect to the reference temperature $T_0 = 273.15K$ and follow the specification as in Marquet (2015). The required constants are defined in Table 4.

Table 4. Constants required for evaluation of atmospheric mass and energy budgets.

Constant	***Value***	***Description***
g	$9.80665 ms^{-2}$	Gravity
T_0	$273.15K$	Reference temperature
c_{pd}	$1004.7\ JK^{-1}kg^{-1}$	Specific heat of dry air at constant pressure
c_{pv}	$1846.1\ JK^{-1}kg^{-1}$	Specific heat of water vapor at constant pressure
$c_{pl} = c_{vl} = c_l$	$4218\ JK^{-1}kg^{-1}$	Specific heat of liquid water
$c_{pi} = c_{vi} = c_i$	$2106\ JK^{-1}kg^{-1}$	Specific heat of ice water
$L_v(T_0)$	$2.501x10^6\ Jkg^{-1}$	Latent heat of vaporization at T_0
$L_f(T_0)$	$0.334x10^6\ Jkg^{-1}$	Latent heat of fusion at T_0
$L_s(T_0)$	$2.835x10^6 Jkg^{-1}$	Latent heat of sublimation at T_0